Crack geometry measurement of steel fiber reinforced concrete based on image analysis

T. Matsumoto
Ph.D., Assoc. Prof., Department of Civil Engineering, The University of Tokyo

M. Nakanishi
Master of Engineering, Tokyo Waterworks Bureau Water Supply Operation Center, Tokyo Metropolitan Government

ABSTRACT: For the crack monitoring of concrete structures, the photographic measurement of crack geometry is carried out. Steel fiber reinforced concrete (SFRC) beams were made and tested under four point flexural loading. SFRC was chosen so that the images of a crack could be captured for a wide range of crack growth stages. Crack images were captured with the use of a microscope that was mounted on an X-Y stage system. Image analysis was executed on the obtained crack images. On the obtained image, edge detection, thinning, border following, and extraction of crack coordinates were conducted. By following these image processes, the coordinates of the crack profiles were obtained. The comparison with displacement gauges show that at large crack opening displacement the difference becomes larger. This is presumably due to concrete inelastic deformation, undetected fine cracks, and the use of long displacement gauge.

1 INTRODUCTION

Crack monitoring of concrete is one of essential items in the maintenance of concrete structures. Crack width, length, and depth are often measured in a periodical manner so that structural degradation processes can be indirectly monitored. The degradation processes that can be possibly monitored include concrete fatigue, alkali silica reaction, freeze-thaw, steel reinforcement corrosion due to chloride attack or carbonation, and unexpected external loads. In addition to crack dimensions, crack pattern can be used for the judgment and identification of a degradation cause, since some degradation processes exhibit a characteristic crack pattern. While a crack is an indicator to show the degradation processes, the development of a crack itself is detrimental, since a crack can be a path of deterioration factors and those factors further promote the degradation processes. Therefore, crack monitoring is important to monitor and rate the condition of degrading concrete structures (JSCE 2005).

Crack monitoring includes the detection and measurement of cracks as well as their time dependent changes. To date, several methods have been proposed and utilized in practice. The simplest method is visual inspection of cracks. This is an easy method; however an inspector has to be close to the surface of a concrete structure. This requires a work at heights in some cases, and it is usually labor intensive. Also, the obtained crack information is point wise, although it is accurate comparatively.

Another method is the use of laser measurement, and it is used especially in a tunnel. The laser irradiation scans the surface of cracked tunnel lining concrete in the circumferential direction, and it measures the distance from the laser source that is located around the center of the tunnel while moving along the longitudinal direction of the tunnel. With the method, the entire tunnel lining surface can be covered, and the width of detected cracks can be measured. However, the development and use of a laser measurement equipment is costly, and this inhibits further applications.

Recently, the technologies of a digital camera have made major advances. The resolution of an image sensing device has increased up to 10 million pixels, and its cost has become reasonable. A camera can capture images at remote location, and it can take images at different magnifications by changing the lenses. Photographic measurement has a versatility, and, with image processes, crack monitoring can be made possible for various concrete structures.

Another concern about crack monitoring is related to advanced computations. In future, it is considered that crack information such as location, dimensions, and pattern will find more applications. This is not only for condition rating, but also for advanced computations. Examples of such computations include a nondestructive test and a durability simulation. As an example of the former case, it is shown that surface crack geometry measurement is used to estimate the steel reinforcement bar stress based on the inverse analysis (Nazmul and Matsumoto 2003a, b, 2004, 2005a, b). For the latter case, accurate durability simulations will certainly require the initial conditions of existing structures, that is, crack information and others.

In this paper, the purpose is to measure the crack geometry with the use of photographic measurement. In the measurement, a microscope system was used in order to obtain the high resolution images. Steel fiber reinforced concrete (SFRC) beams were tested to obtain crack images under stable crack growth. Image processes were carried out to obtain the coordinates of a crack for the usage in finite element analysis. Finally, comparison with displacement gauge measurement was made. The accuracy is assessed, and the error causes are discussed.

2 STATIC FLEXURAL EXPERIMENT OF SFRC BEAMS

2.1 *Materials and specimens*

Static flexural experiment of steel fiber reinforced concrete (SFRC) beams was conducted in order to obtain crack images. The use of SFRC was chosen to capture crack images for a wide range of crack growth stages. It is the characteristic of SFRC that SFRC beams exhibit a gradual crack growth due to fiber bridging action across a crack, and this experiment takes advantage of this characteristic by mixing steel fibers at the fiber volume fraction of 2%.

Fiber properties are shown in Table 1, and the mix proportion of SFRC is shown in Table 2. The water to cement ratio is 50%, and the maximum coarse aggregate size is 20 mm. 11 beams with 40 cm length, 10 cm height, and 10 cm thickness and six cylinders with 10 cm diameter and 20 cm height were made. The specimens were demolded at one day after mixing, and they were cured in water for at least 21 days.

Compression strength was measured with cylinders at 21 days and 70 days, and they were 50.3 MPa and 56.7 MPa respectively.

Table 1. Fiber properties

Diameter	Length	Tensile strength
mm	mm	MPa
0.6	30	1142

Table 2. Mix proportion of SFRC in kg/m3. W: water, C: cement, FA: fine aggregate, CA: coarse aggregate, AD: air entraining and water reducing agent, and SF: steel fiber.

W	C	FA	CA	AD	SF
205	410	998	545	1.025	157

2.2 *Experimental setup*

Figure 1 shows the experimental setup. SFRC beams were tested under four point flexural loading. Two displacement gauges with the gauge length of 10 mm were attached on the bottom face of the beams in order to measure the gauge displacement that includes crack opening displacement. Specimens were painted white to get adequate contrast between cracked and non-cracked zones, so that the image analysis of digital images was facilitated.

Four point flexural loading was applied under the displacement control of 0.005 mm/s with a feed back controlled loading machine. Load and stroke displacement were recorded, and the displacements were also recorded with the two displacement gauges.

Loading was paused, and the displacement was kept constant at prescribed displacement values: 0.50, 0.55, 0.60, 0.65, 0.70, 075, 0.80, 0.85, 0.90, 0.95, 1.00, 1.05, 1.10, 1.15, 1.20, 1.25, 1.30, 1.35, 1.40, 1.45, 1.50, 1.60, 1.80, 2.00, 2.50, 3.00, and 4.00. Upon the crack occurrence, a microscope was employed to capture the crack image during each load pausing time.

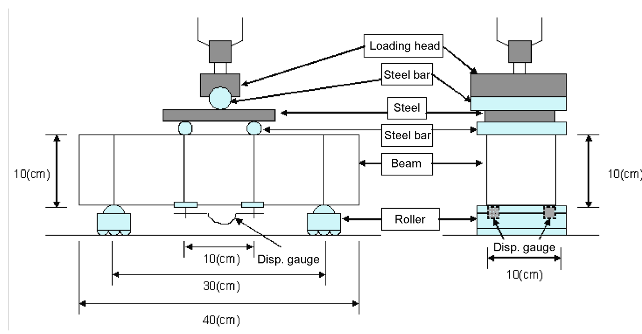

Figure 1. Experimental setup

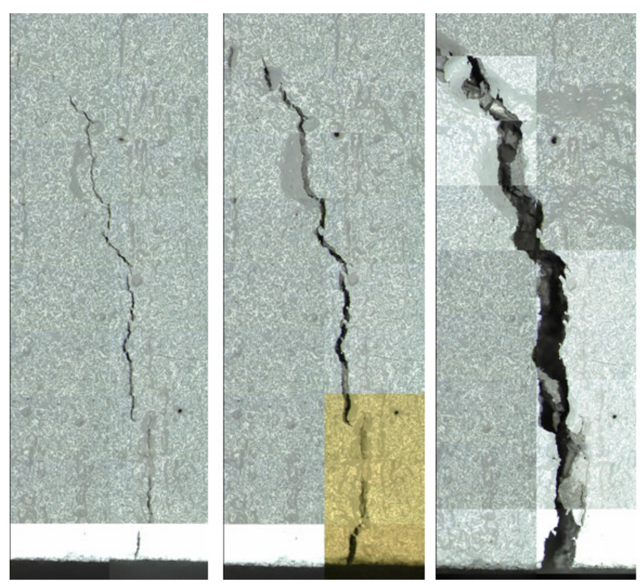

Figure 2. Example images of a growing crack

2.3 *Image acquisition*

A microscope of 100 times power that was mounted on an X-Y stage system was used to capture and record the crack on the specimen side surface. The rectangular area of 10 cm width and 10 cm height in the center beam span was divided into frames, each of which was 640 x 480 pixels. The rectangle image was assembled with the frames by cutting the overlapping portions of neighboring frames. Example images of a growing crack are shown in Figure 2

3 IMAGE ANALYSIS

3.1 *Flow of image analysis*

The purpose of this study is to measure the crack geometry, namely, starting from an original digital image, to obtain the crack coordinates finally. The flow of image analysis is shown in Figure 3. The details of image analysis are explained below (Sakai 2002).

3.2 *Edge detection*

A crack is expressed as a set of dark pixels compared to surrounding pixels, and usually a differential type of filter that detects the profile or the edge of an object is used. In the current study, wavelet transform is utilized to detect the edge of a crack. After the transform, the image is filtered with a threshold value.

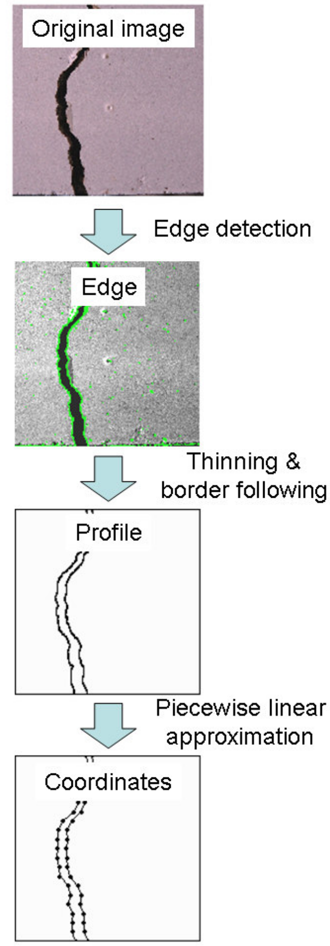

Figure 3. Flow of image analysis

3.3 *Thinning*

The edge of a crack has a width of several pixels usually, therefore thinning process is applied in the horizontal direction, which is approximately the perpendicular direction of the crack.

3.4 *Border following*

After thinning process, the pixels forming a crack profile are selected. This is done by border following process. A pixel at the crack mouth is selected as a starting point, and the closest pixel is followed subsequently. By this border following process, pixels that do not form the crack profile will be deleted.

3.5 *Extraction of crack coordinate*

The crack profile is a series of pixels. In the final process, the profile is approximated as a piecewise linear line. In this study, the beam height of 10 cm is divided into 40 points, and, at the interval of 2.5 mm, the coordinates of each point is selected.

4 CRACK GEOMETRY MEASUREMENT

4.1 *Extraction of crack coordinates*

Experimentally obtained load-displacement relation of an SFRC beam is shown in Figure 4. The initial gradual rise of the load-displacement curve is due to machine setting. As designed, the SFRC beam exhibited gradual load increase even after cracking, and also gradual softening after the peak was observed. The crack appeared as a single crack on the bottom face of the beam, and later bifurcated into a few cracks.

The digits in Figure 4 show the point of image acquisitions. At each point, the loading was paused while displacement was kept at a prescribed value, and the microscope scanned the center beam span.

As described previously, the crack images were processed: edge detection, thinning, border following, and extraction of crack coordinates. Figure 5 shows the extracted crack coordinates; only the coordinates at point 1, 3, 5, 7, and 9 are shown. In order to follow the both crack profiles, a different start pixel was selected for each crack profile.

The crack growth of the SFRC beam is summarized below. At Point 1 which corresponds to 2.67 ton, the crack has already initiated and grown to 20 mm. Point 3 is just before the peak load of 2.81 ton, and the crack has grown up to 65 mm. The crack growth up to the peak load is remarkable, while the growth after the peak is not so big. After Point 5, the crack grew only from 72 to 78 mm.

4.2 *Comparison with displacement gauge*

Based on the extracted crack coordinates of both crack profiles, the crack opening displacement (COD) can be computed. This COD is compared with the displacement gauge measurement on the bottom face of the center beam span in order to evaluate the accuracy of the geometry measurement based on the image analysis.

Figure 6 shows the comparison of COD between image analysis and displacement gauge measurement on the load-displacement relation. And Figure 7 also shows the comparison of COD, but it shows the crack profile from the side surface.

The displacement gauge measurement is adjusted so that the concrete elastic deformation inside the gauge length is excluded. The secant elastic modulus of 32.5 MPa which is obtained from the average of compression tests is used.

Although the elastic deformation is excluded from the gauge measurement, the difference of 0.06-0.2 mm is observed. The measurement based on the image analysis always underestimates the COD, and the difference becomes larger as the crack grows and opens up.

In Figure 7, it is seen that the crack profile measured based on the image analysis becomes less erroneous. Since one pixel corresponds to about 5 µm, the crack profile becomes reasonably accurate around the COD of 0.5 mm, which corresponds to 100 pixels.

The difference from the displacement gauge measurement is presumably due to concrete inelastic

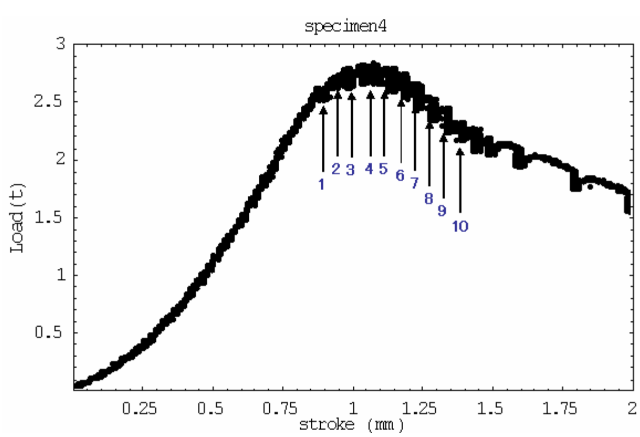

Figure 4. Load-stroke displacement relation and image acquisition points

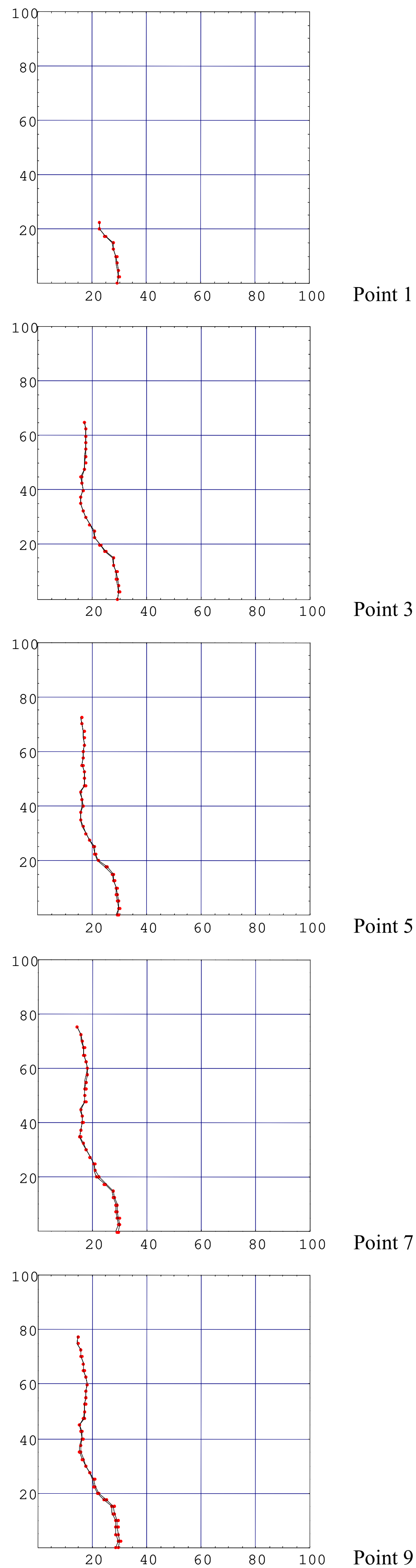

Figure 5. Extraction of crack coordinates

deformation, undetected fine cracks, and the use of long displacement gauge.

5 CONCLUDING REMARKS

In the context of the crack monitoring of concrete structures, the photographic measurement of crack geometry has been carried out. The geometry measurement is intended not only for condition monitoring and rating, but also for advance computations such as nondestructive tests and durability simulations.

Steel fiber reinforced concrete (SFRC) beams with 40 cm length, 10cm height, and 10cm thickness were made and tested under four point flexural loading. SFRC was chosen so that the images of a crack could be captured for a wide range of crack growth stages. It is the characteristic that SFRC beams exhibit a gradual crack growth due to fiber bridging action across a crack.

Crack images were captured with the use of a microscope of 100 times power that was mounted on an X-Y stage system. The side surface of center beam span was recorded with multiple frames of 640 x 480 pixels. Crack images were successfully obtained, including the points before and after the load peak.

Image analysis was executed on the obtained crack images. After the frames were assembled into one image, edge detection, thinning, border following, and extraction of crack coordinates were conducted. By following these image processes, the coordinates of the crack surfaces were obtained.

The comparison with displacement gauges show that at large crack opening displacement the difference becomes larger. This is presumably due to concrete inelastic deformation, undetected fine cracks, and the use of long displacement gauge. It is necessary to use a shorter displacement gauge and to include the deformation of concrete inelasticity and fine cracks.

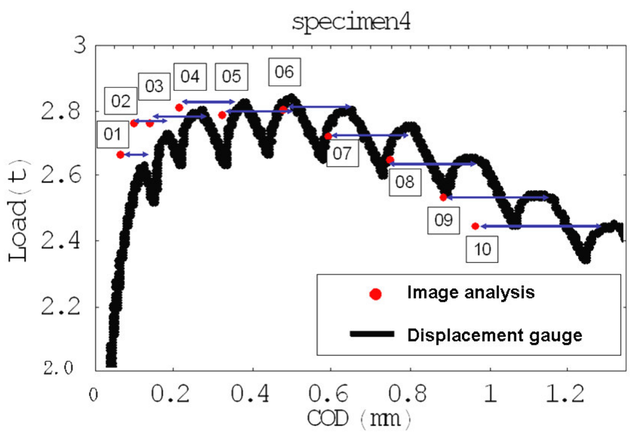

Figure 6. Load-crack opening displacement (COD) relation and comparison of crack opening displacement between image analysis and displacement gauge measurement

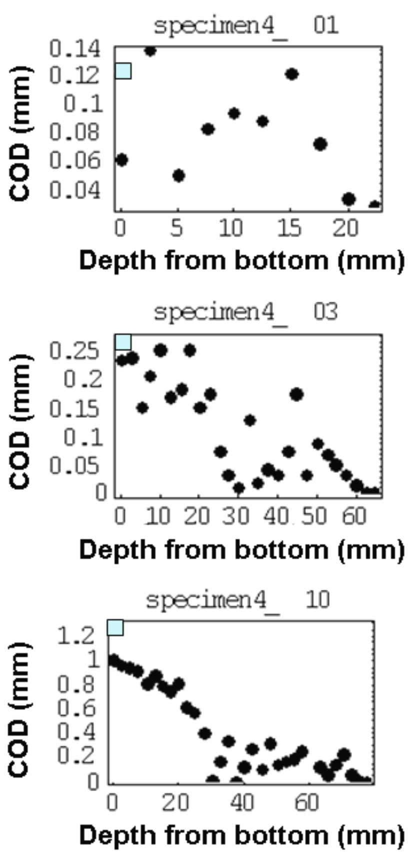

Figure 7. Comparison of crack opening displacement between image analysis (circle) and displacement gauge measurement (square).

REFERENCES

JSCE 2005. *JSCE Guidelines for Concrete No.4 Standard Specifications for Concrete Structures -2001 "Maintenance."* JSCE.

Nazmul, I. M. & Matsumoto, T. 2003a. Determination of Steel Stresses in Reinforced Concrete Structures from Crack Opening Profile, In Z. Wu & M. Abe (eds), *Structural Health Monitoring and Intelligent Infrastructure*: 739-746. Balkema.

Nazmul, I. M. & Matsumoto, T. 2003b. Inverse Analysis to Determine Crack Bridging Stresses in Fiber Composites. *JSCE Journal of Applied Mechanics* 6: 1097-1104.

Nazmul, I. M. & Matsumoto, T. 2004. Inverse Analysis to Determine Re-bars' Force from External Crack Widths Measurement. *JSCE Journal of Applied Mechanics* 7: 1179-1186.

Nazmul, I. M. & Matsumoto, T. 2005a. Inverse Analysis of Measured Crack Widths for Reinforcing Steel Stress. *submitted for Journal of Engineering Mechanics*.

Nazmul, I. M. & Matsumoto, T. 2005b. Regularization of Inverse Problems in Reinforced Concrete Fracture. *submitted for Journal of Engineering Mechanics*.

Sakai, K. 2002. *Introduction to Digital Image Analysis*. CQ Publishing. (In Japanese)